SPE/DOE 9870

SPE/DOE
Society of Petroleum Engineers
U.S. Department of Energy

THE RELATIONSHIP OF PERMEABILITY TO CONFINING PRESSURE IN LOW PERMEABILITY ROCK

by James B. Jennings, *Herbert B. Carroll, *Clarence J. Raible,
Bartlesville Energy Technology Center
*Members SPE-AIME

This paper was presented at the 1981 SPE/DOE Low Permeability Symposium held in Denver, Colorado, May 27-29, 1981. The material is subject to correction by the author. Permission to copy is restricted to an abstract of not more than 300 words. Write SPE, 6200 North Central Expressway, Dallas, Texas 75206.

ABSTRACT

Laboratory permeability measurements of low permeability (less than 1 md) reservoir rock is significantly affected by test confining pressure. Knowledge of the confining pressure is required to predict permeability at reservoir conditions. A model is proposed which relates electrical conductivity, permeability, and pore dimensions to confining pressure. The model assumes that rock pores are interconnected by thin cracks and microfractures which can be modeled by rectangular slits. For this model, core permeability is related to confining pressure by a third order polynomial, and electrical conductivity is related to confining pressure by a first order polynomial. Electrical conductivity and permeability versus confining pressure measurements were made on test cores having laboratory Klinkenberg permeabilities from 20 to 200 microdarcys. The experimental measurements were found to be consistent with the slit model theory.

INTRODUCTION

Thomas and Ward[1] have shown that the measured permeability of many western gas sandstone cores is significantly decreased by increased test confining pressure, whereas effective porosity is only slightly affected. Jones and Owens[2] developed an empirical method for relating permeability to confining pressure which is valid for a variety of low-permeability western gas sandstone core. The results are consistent enough to suggest that a rock matrix model can be developed to relate pore geometry to laboratory permeability. Their studies suggest that low-permeability reservoir rock consists of a matrix material containing larger pores which contribute mostly to the rock porosity. The larger pores are interconnected by smaller pore throats that restrict permeability and are easily deformed by changes in confining pressure.

Wyllie and Gardner[3] developed a capillary model in which pores and pore throats are assumed to be short sections of capillary tubes. Stacking sections of the capillary tubes together in a random manner forms a model which can relate porosity, electrical conductivity, and permeability. Archie's equation is often inferred from the Wyllie-Gardner model. It is possible to extend the capillary model to include the effects of confining pressure. The extension is made by assuming that each capillary tube is a thick-walled cylinder to which the confining pressure is applied. As the confining pressure is increased, the inside diameter of the capillary is reduced which reduces the permeability and electrical conductivity. This model could be useful if the pore throats were nearly round capillary tubes. It is more likely that pore throats in low-permeability sands can be described better as slits, cracks or micro-fractures. For the same cross-section area, a slit will be a much weaker structure than a capillary tube and will undergo a larger change in area due to an applied external stress. Our paper proposes that a slit model can describe the effect of confining pressure on permeability and electrical conductivity for low permeability reservoir rock.

Slit Model Theory

The following assumptions have been made for the model: (1) Flow paths through the core are independent and consist of a series of pores connected by rectangular slits. (2) The slits are uniform in size in each flow path. (3) Permeability and electrical conductivity are limited primarily by slit dimensions and fluid properties. (4) Viscous flow is assumed; slit entrance and surface roughness effects are neglected.

References and illustrations at end of paper.

(5) The bulk rock properties are approximated by the classical theory of elasticity. (6) Slits are sparcely distributed in any rock cross section so their stress fields do not interact.

If the stress field for a typical slit is known, the deformation due to a change in stress can be determined, and the geometry of the slit can be related to permeability and electrical conductivity. In a typical laboratory test, the confining pressure is applied to a cylindrical core plug hydrostatically. It can be shown that radial and tangential stresses produced in the core plug are

$$\sigma_r = \sigma_\theta = -P_c \quad \ldots . \quad (1)$$

The radial and tangential stresses in equation (1) are acting along the principal stress directions within the test sample. Obviously these are not necessarily the principal stress directions of the in situ stress field. The error caused by this difference will be a function of the anisotropy of the rock and the magnitude and directions of the in situ stress components. Only the stresses as they exist in the test plug will be considered in this paper.

Figure 1 shows a theoretical slit which is centered on a core radius R and is inclined by the angle ψ from R. AA' represents a plane parallel to the w_i, ℓ_i plane of the slit.

The forces acting on plane AA' directly above slit i will be

$$f_r = \ell_i \, w_i \, \sigma_r \sin \psi \quad \ldots . \quad (2a)$$

and

$$f_\theta = \ell_i \, w_i \, \sigma_\theta \cos \psi \quad \ldots . \quad (2b)$$

The total force normal to the plane AA' and directly above slit i will be

$$f_i = \ell_i \, w_i \, \sigma_i = \ell_i \, w_i \, \sigma_r \sin^2 \psi + \ell_i \, w_i \, \sigma_\theta \cos^2 \psi \quad \ldots . \quad (3)$$

Making use of equation (1) and a trigonometric identity gives the useful result

$$\sigma_i = \sigma_r = \sigma_\theta \quad \ldots . \quad (4)$$

Plane AA' is far enough from the slit so that σ_i is nearly constant along the width of the slit. Therefore, σ_i is a representative stress which acts to deform any particular slit in the core plug cross section.

Figure 2 illustrates the distortion of a single slit due to the stress field σ_i. The matrix material between AA' and the slit forms a single layer structure or beam which has fixed ends and uniform loading. The deflection of the beam is given by Obert[4].

$$\eta = \frac{\sigma_i \, x^2}{24 \, E \, I_y} (w - x)^2 \quad \ldots . \quad (5)$$

The slit height at any point is

$$d = h - K_d \, P_c \, x^2 \, (w - x)^2 \quad \ldots . \quad (6)$$

where

$$K_d = \frac{2}{24 \, E \, I_y} \quad \ldots . \quad (7)$$

The effect of tri-axel stress on the slit could be included in the analysis as an increase in K_d by Poisson's ratio. The effect of confining stress on slit width, w, is small and has been neglected.

The area of the slit is

$$s = \int_0^w d \, dx = w(h - K_d \, P_c \, w^4/30) \quad \ldots . \quad (8)$$

The electrical conductance of a single slit filled with conductive liquid will be

$$G_{si} = \frac{A_{si}}{R_w \, \ell_i} \quad \ldots . \quad (9)$$

The total electrical conductance of the core may be obtained by substituting (8) into (9) and summing over all slits.

$$G = \frac{1}{R_w} \sum_{i=1}^{N} \frac{w_i \, h_i}{\ell_i} - \frac{P_c \, K_d}{R_w \, 30} \sum_{i=1}^{N} \frac{w_i^5}{\ell_i} \quad \ldots . \quad (10)$$

Equation (10) can be rewritten in the linear form

$$G = B_o + B_1 \, P_c \quad \ldots . \quad (11)$$

Thus for the slit model the electrical conductivity will be a linear function of the confining pressure.

The form of the equation for fluid flow through a slit as shown in Figure 2 can be found from Poiseuille's equation for viscous flow through a capillary by using dimensional analysis. Poiseuille's equation is

$$Q = \frac{\pi r^4 \Delta p}{8 \mu \ell} \quad \ldots . (12)$$

The assumption for viscous flow in a slit is that Q must be proportional to w. For the slit flow equation to be dimensionally correct

$$Q_s = \frac{K_s \Delta p \, d^3}{\mu \ell} w \quad \ldots . (13)$$

K_s is the constant for slits and is known[5] to be 1/12. For a differential section of the slit the flow will be

$$dQ = \frac{K_s \Delta p \, d^3}{\mu \ell} dx \quad \ldots . (14)$$

The total flow through a distorted slit will be

$$Q_s = \frac{K_s \Delta p}{\mu \ell} \int_0^w d^3 dx \quad \ldots . (15)$$

by placing equation (6) into (15), the following equation is obtained:

$$Q_s = \frac{K_s \Delta p}{\mu \ell} \left[h^3 w - \frac{h^2 K_d w^5}{10} P_c + \frac{h K_d^2 w^9}{210} P_c^2 - \frac{k_d^3 w^{13}}{12012} P_c^3 \right] \quad \ldots . (16)$$

Equation (16) gives the flow for one flow path. The total flow through the core will be the sum for all flow paths in the core cross section. The total flow can also be found by Darcy's law

$$Q = \frac{k \Delta p A}{L} \quad \ldots . (17)$$

Equating the total slit flow with the core flow from Darcy's law and solving for the permeability k gives

$$k = \frac{K_s L}{A} \left[\sum_{i=1}^{N} \frac{h_i^3 w_i}{\ell_i} - P_c \sum_{i=1}^{N} \frac{h_i^2 K_d w_i^5}{10 \ell_i} + P_c^2 \sum_{i=1}^{N} \frac{h_i K_d^2 w_i^9}{210 \ell_i} - P_c^3 \sum_{i=1}^{N} \frac{K_d^3 w_i^{13}}{12012 \ell_i} \right] \quad \ldots . (18)$$

All the terms in the summations are constant for a given core so equation (18) may be written

$$k = A_o + A_1 P_c + A_2 P_c^2 + A_3 P_c^3 \quad \ldots . (19)$$

From experimental data of electrical conductivity and permeability versus net confining pressure, the A and B coefficients in equations (11) and (19) may be found. With appropriate assumptions it may be possible to make estimates of h, w and ℓ.

EXPERIMENTAL PROCEDURE

Four cores from Mapco RBU 11-17F in Uintah County, Utah and four cores from Wexpro #1 Mesa Unit in Sublette County, Wyoming were tested. The core plugs were cut parallel to the bedding plane and were nominally 2.5 cm in diameter and length. The cores were vacuum saturated with 8 percent KNO_3 and 0.02 percent NaN_3. The KNO_3 solution was used as a pore fluid primarily to minimize corrosion problems during the experiments. The NO_3 ions also provide minimum pH and clay adsorption changes from those of the original pore fluids. The potassium ion provides improved clay stabilization and the NaN_3 was the anti-bacterial agent.

The cores were tested at ambient temperature of 24° C in a Core Labs pressure vessel modified for electrical conductance measurements. The pore fluid pressure was maintained at 0.69 MPa (100 psi) across the core using a nitrogen driven transfer cylinder. The confining pressure was the principal independent variable in the study and was increased from 2.07 MPa to 28.98 MPa (300 psi to 4200 psi) during the tests. Liquid permeabilities were determined from time and weight measurements of fluid passing through the core. Electrical conductance measurements were made at 10 kHz using a Hewlett Packard 4262A LCR meter. About 5 pore volumes of fluid were allowed to pass through the core before measurements were begun. For each confining pressure, permeability and conductivity measurements were made at 1 hour intervals until stable results were obtained.

Data Analysis

The pore pressure helps support the sides of the slit so the net confining pressure was defined as

$$P_c = P_m - \bar{p} \quad \ldots . (20)$$

The input pore pressure was 0.69 MPa (100 psi) and the output was 0.0 MPa so that the mean pore pressure $\bar{p}$ was 0.34 MPa (50 psi).

Permeability versus net confining pressure data were fit to third order polynomials using a least-squares fit by the method and computer programs described by Carnahan, et al[6].

CONCLUSIONS

Typical permeability data and their fitted curves are shown in Figures 3 and 4.

Table 1 gives the coefficients and standard deviations for the fitted third-order polynomial equation (19). The results demonstrate that a third-order polynomial can easily fit the permeability data. The largest standard deviation between the experimental data and the fitted polynomial is only 3 percent of the unstressed value. The signs of the polynomial coefficients given in equation (18) agree with all of the calculated values in Table 1. However, polynomials can fit data from a variety of processes where other functions are the perferred models. Fitted polynomials are also poor predictors when the value of the independent variable is outside the range of experimental data.

Electrical conductivity data for two of the core plugs are shown in Figure 5. The data plot either as a shallow curve or as straight line segments. A line segment interpretation is consistant with equation (11) and the slit theory if we allow some slits or microfractures to close completely as confining pressure is increased. Slit closure is not apparent in the permeability data since larger slits which support most of the fluid flow do not close.

The data were also plotted using the Jones-Owens method (cube root of permeability vs. logarithm of net confining pressure) in Figure 6. The data do form straight lines for net confining pressures above 6.9 MPa (1000 psi) as observed by Jones and Owens. The Jones-Owens method is easier to apply and is more useful for making permeability predictions than the polynomial model. But the polynomial model provides a mechanism to describe how the internal rock structure could be changing with applied stress. With added assumptions, the dimensions of an equivalent slit could be determined. In addition, the slit model fits the data for confining pressures below 6.9 MPa (1000 psi).

Since an actual reservoir rock does not contain pores interconnected by rectangular slits, the model should provide some reasonably equivalent response or interpretation to be useful. Two equivalences are suggested. First, the relatively weak structure of the rectangular slits is comparable to the weakness of irregular pore openings, small cracks and microfractures, which are assumed to limit the permeability and electrical conductivity in low permeability rock. Second, the model coefficients are functions of dimensions which should be comparable to actual pore measurements.

NOMENCLATURE

d = height of slit at point x

f_i = total force normal to slit i

f_r = radial force acting on slit

f_θ = tangential force acting on slit

h = height of slit when unstressed

i = subscript for slit number

k = permeability

ℓ = length of slit

$\bar{p}$ = mean pore pressure

r = capillary radius

w = width of slit

x = dimension along width of slit

A = area of core plug

A_0, A_1, A_2, A_3 = coefficients of cubic equation relating permeability to net confining pressure

A_s = area of slit

B_0, B_1 = coefficients of linear equation relating electrical conductivity to net confining pressure

E = Young's modulus

G = electrical conductance of saturated rock

G_s = electrical conductance of slit

I_y = moment of inertia of beam

K_d = constant relating beam deflection to stress

K_s = viscous flow constant for slit

L = core plug length

N = number of slits in cross section

P_c = net confining pressure

P_m = gage pressure of confining fluid

Q = core plug flow rate

Q_s = slit flow rate

R = radius of core plug

R_w = resistivity of saturating fluid

Δp = core flow pressure differential

η = deflection of beam under uniform stress

μ = fluid viscosity

σ_i = stress normal to plane of slit i

σ_r = radial stress component in core plug

s_Θ = tangential stress component in core plug

ψ = slit inclination angle with radius

REFERENCES

1. Thomas, R. D. and Ward, D. C.: "Effect of Overburden Pressure and Water on Gas Permeability of Tight Sandstone Cores," J. Pet. Tech., February, 1972, pp. 120-124.

2. Jones, F. O. and Owens, W. W.: "A Laboratory Study of Low Permeability Gas Sands," SPE Technical Paper 7551.

3. Wyllie, M. R. J. and Gardner, G. H. F.: "The Generalized Kozeny-Carman Equation," World Oil, April, 1958, pp 210-228.

4. Obert, L. and Duval, W. I.: "Rock Mechanics and the Design of Structures in Rock," John Wiley, New York, NY, 1967, pp 148-149, 519.

5. Amyx, J. W., Bass, D. M., and Whiting, R. L.: "Petroleum Reservoir Engineering," McGraw Hill, New York, NY, 1960, pp 84-85.

6. Carnahan, B., Luther, H. A. and Wilkes, J. O.: "Applied Numerical Methods," John Wiley, New York, NY, 1969, pp 578-584.

TABLE 1. Polynomial coefficients for least-square fit to permeability versus net confining pressure measurements. Datum for confining pressure is in psi and permeability is in micro-darcys.

Core	A_0	A_1	A_2	A_3	Standard Deviation
U8358.7	266.9	-233.5	74.84	-8.73	7.36
U8290.9	103.2	- 98.0	34.66	-4.12	2.34
U8358.3	48.3	- 46.01	16.17	-1.93	1.01
U8365.4	17.9	- 15.2	4.75	- .517	0.30
W9179.5	19.4	- 13.2	3.61	- .352	0.37
W5204.8C	77.0	- 27.4	7.33	- .726	1.10
W5210.8A	67.8	- 26.7	8.19	- .970	1.04
W9176.5	19.1	- 17.1	5.20	- .512	0.60

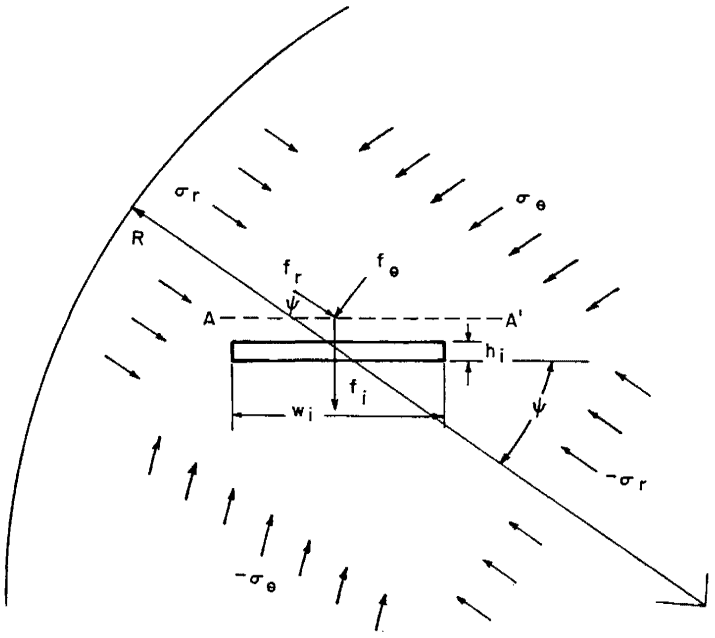

Fig. 1 - Forces acting on a rectangular slit in a cylindrical core plug with hydrostatic loading.

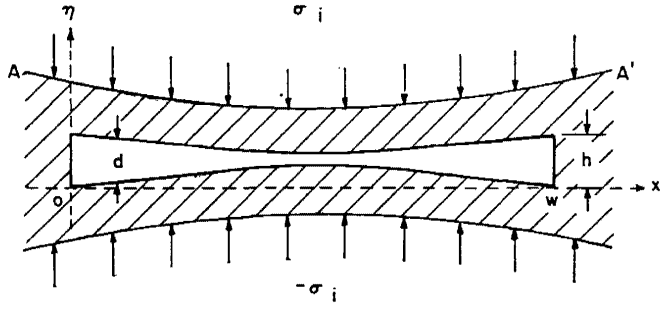

Fig. 2 - Distortion of a rectangular slit cross-section by a uniform stress field. Cross-section is normal to the flow path.

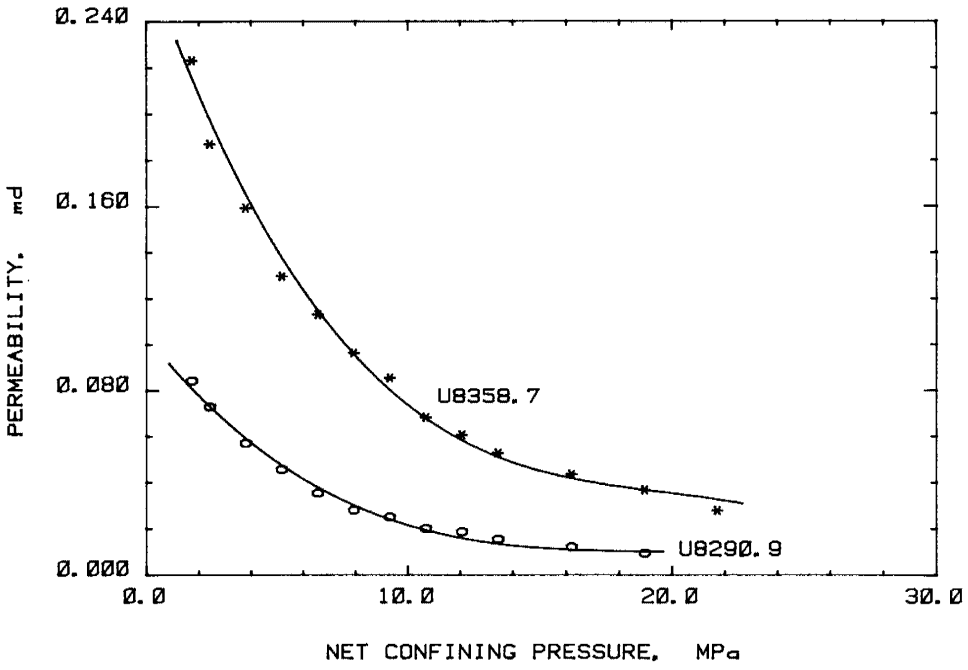

Fig. 3 - Effect of confining pressure on permeability of Uintah County, Utah core material. Solid lines are least-squares polynomial fits.

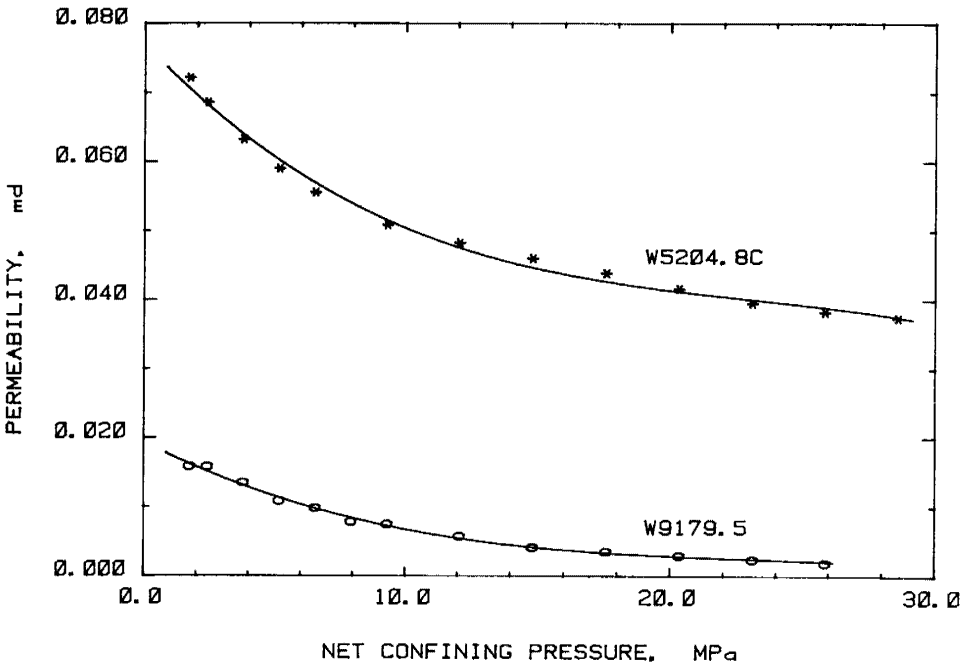

Fig. 4 - Effect of confining pressure on permeability of Sublett County, Wyoming core material. Solid lines are least-squares polynomial fits.

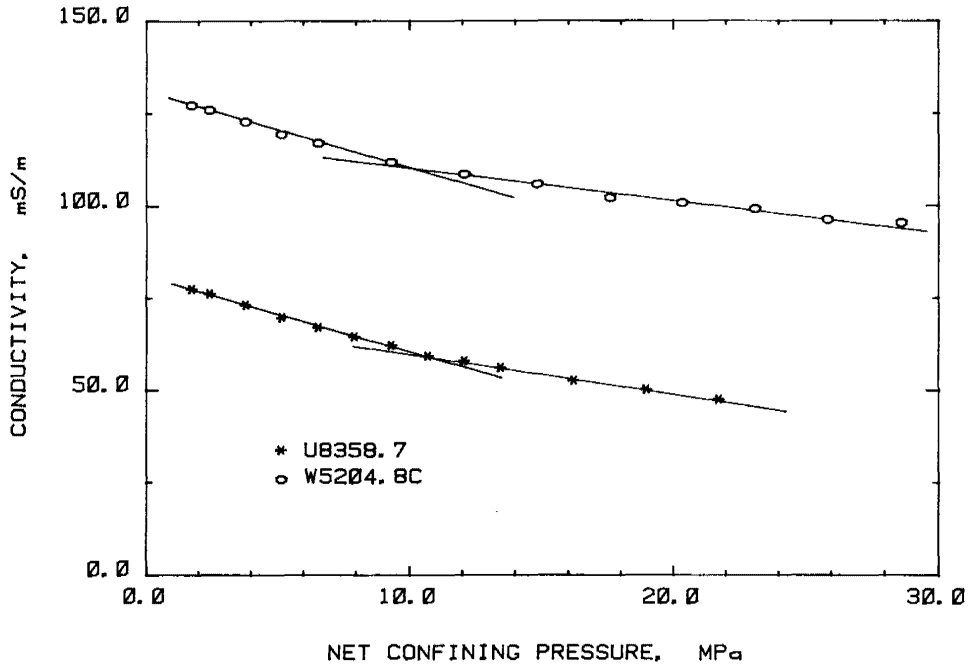

Fig. 5 - Effect of confining pressure on electrical conductivity.

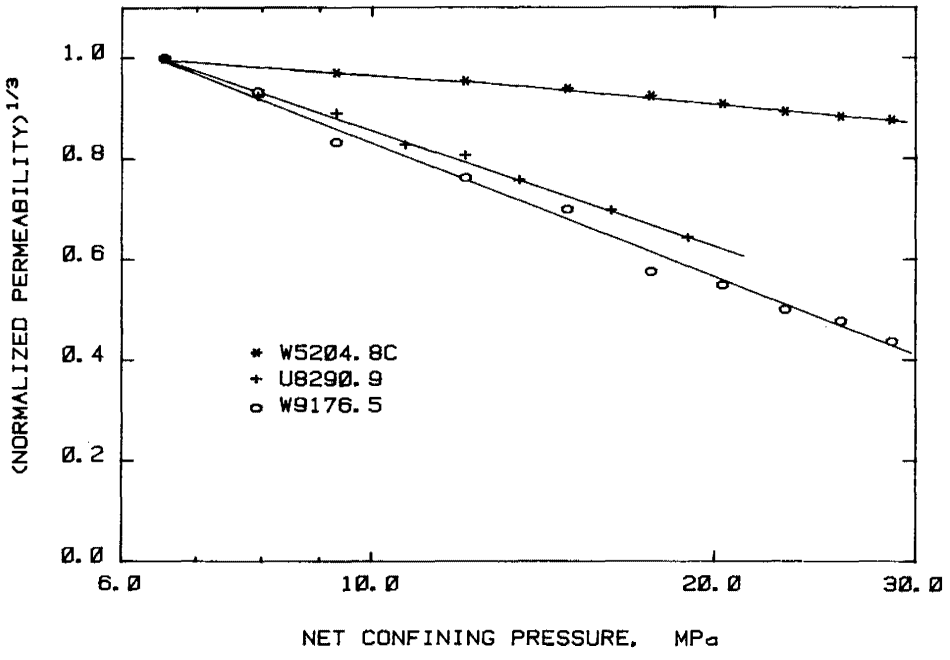

Fig. 6 - Jones-Owens plot for relating permeability to confining pressure.